



**ARTICLE**

# The Promoting Effect of Multifunctional Groups on the Thermal and Mechanical Properties of PVC Materials

Mei Wang<sup>1,\*</sup>, Xinzhu Fan<sup>1</sup>, Xianghai Song<sup>2</sup> and Quan Bu<sup>1,\*</sup>

<sup>1</sup>School of Agricultural Engineering, Jiangsu University, Zhenjiang, 212013, China

<sup>2</sup>Institute of the Green Chemistry and Chemical Technology, School of Chemistry and Chemical Engineering, Jiangsu University, Zhenjiang, 212013, China

\*Corresponding Authors: Mei Wang. Email: 1000004927@ujs.edu.cn; Quan Bu. Email: qbu@ujs.edu.cn

Received: 04 April 2022 Accepted: 06 June 2022

## ABSTRACT

The development of PVC materials grafted with mannich base originated from myrcene (P-MAM-g, where the mannich base derived from myrcene is abbreviated as MAM) via green and effective synthetic methods is a good strategy to avoid unacceptable discoloration and deterioration of thermal and mechanical properties caused by autocatalytic dehydrochlorination (DHC) during PVC processing. In this study, MAM with double bonds, amino groups, ester groups, and phospholipid groups was introduced into the chains of PVC to improve the thermal stability of PVC. The experimental results showed that the covalent attachment of MAM to PVC enhanced both the initial and the long-term stability of PVC. The enhanced performance of P-MAM-g compared with unmodified PVC is attributed to the simultaneous introduction of double bonds and amino groups into the PVC structure. The double bonds trapped the unstable chlorine atoms originated from the degradation of the PVC chain and reacted with the labile macromolecular radicals originated from PVC, thus inhibiting the radical degradation of the PVC chain. Furthermore, the amino groups absorbed the HCl produced in the degradation of PVC, inhibiting the adverse effects of HCl. P-MAM-g displayed better intrinsic flexibility and anti-migration ability of organic functional components compared with the control PVC materials. A possible stabilizing mechanism of the P-MAM-g was also presented.

## KEYWORDS

Myrcene; poly(vinyl chloride); covalent grafting; self-stabilization

## Nomenclature

Term 1: Interpretation 1

Term 2: Interpretation 2

## e.g.

∅: Porosity

s: Skin factor



## 1 Introduction

Poly(vinyl chloride) (PVC) has been widely applied in various fields; however, it degrades easily at processing temperatures due to autocatalytic dehydrochlorination (DHC) [1,2]. This degradation occurs because of the elimination of HCl and the production of conjugated unsaturated double bonds [3], which remarkably decreases the color, thermal and mechanical properties [4,5]. Previous studies have shown that adding thermal stabilizers is an effective and practical method to inhibit the degradation of PVC [6].

Metallic soaps, organic tin/lead salts, and nitrogenous compounds have been recently used as thermal stabilizers and color retention reagents for PVC [7–9]. Though lead salts and organic tin can effectively stabilize PVC, the toxicity limits their application in PVC products.  $\text{CaSt}_2/\text{ZnSt}_2$  (calcium stearate/zinc stearate) composite heat stabilizers have been extensively investigated attributing to their synergistic effect in stabilizing PVC. However, zinc chloride ( $\text{ZnCl}_2$ ) with strong Lewis acidity is formed in the manufacturing process of PVC materials thermally stabilized by  $\text{CaSt}_2/\text{ZnSt}_2$ , causing an unfavorable “zinc burning” phenomenon [1,10]. Organic thermal stabilizers show great potential attributing to their advantages including high efficiency, low environmental impact, good compatibility, and strong universality. However, existing organic thermal stabilizers fail to inhibit long-term discoloration of PVC and need to be used in conjunction with other thermal stabilizers for further enhancing thermal stability [11].

PVC materials are currently prepared by physically blending thermal stabilizers with PVC, causing uneven dispersion of the thermal stabilizers and the migration of organic functional components [12]. This process deteriorates their thermal stability [13]. Therefore, the development of non-toxic and green, uniformly dispersed and anti-precipitated organic thermal stabilizers is of great significance to the development of thermally stable PVC materials.

In comparison with physical blending, the introduction of organic functional groups into the structure of PVC via chemical grafting is expected to significantly improve the migration resistance abilities and mechanical properties of PVC. For example, Jia et al. [14] prepared cardanol butyl ester mannich base with cardanol and grafted it onto PVC via a substitution reaction. The as-obtained PVC sample displayed good plasticizing and mechanical properties and a migration rate almost of 0. Although PVC materials grafted with organic compounds present improved long-term thermal stability compared with pure PVC, it is still difficult to simultaneously delay “zinc-burning” and inhibit the initial degradation and coloring of PVC materials. For instance, Zhu et al. [15] successfully inhibited the first stage of thermal degradation of PVC by grafting phenol to PVC under microwave irradiation, resulting in improved long-term thermal stability of the PVC. However, the initial color and prolonged long-term thermal stability of the as-prepared PVC products were still not sufficient compared with commercial PVC samples. In addition, the flexibility of the PVC sample was not satisfactory due to the rigid structure of phenol, thus the sample exhibited poor mechanical properties. Therefore, it is still urgent to develop novel organic thermal stabilizers by means of a grafting strategy to further facilitate the initial stability, long-term stability, and mechanical properties of PVC materials.

Recently, it was reported that Ca/Zn stabilizers with multifunctional groups such as amino groups, double bonds, and ester groups were reported to endow PVC with good long-term stability [16,17]. These functional groups can trap the labile chlorine atoms removed from the PVC chain, react with the unstable macromolecular radical of PVC, and act as HCl absorbers at subsequent stages of degradation, demonstrating a significant thermal stabilizing effect on PVC. Thus, PVC samples grafted with organic compounds containing amino groups, double bonds, and ester groups are expected to display enhanced stability and thus improved mechanical properties. Myrcene, an oily liquid, contains conjugated double bonds in its structure and thus is an ideal raw material for the preparation of multifunctional PVC materials. The conjugated double bond of myrcene enables it to react easily with dienophiles via the Diels–Alder reaction to introduce other functional groups into its structure. The as-obtained products

from this reaction of myrcene have been widely applied in coatings, epoxy curing agents, and vinyl ester resin [18–20]. Similarly, the introduction of lauraldehyde derivatives into the PVC chains via covalent bonds is a promising choice for constructing self-stabilized PVC polymers.

Accordingly, this study describes the development of a myrcene-based organic thermal stabilizer containing double bonds, amino groups, ester groups, and phospholipid groups in its structure and its application in stabilizing PVC via chemical grafting. A series of MAM grafted PVC samples (P-MAM-g, where the mannich base derived from myrcene is abbreviated as MAM) were successfully prepared by the replacement reaction of the chlorine group in PVC with a mannich base derived from myrcene. To date, there are no reports of PVC materials simultaneously incorporating double bonds, amino groups, ester groups, and phospholipid groups into their structure.

## 2 Experimental Section

### 2.1 Materials

Myrcene was purchased from Jiangxi Global Natural Spices Co. (China), containing about 79% of myrcene. Acrolein (98%, Aladdin), diethyl phosphite (99%, Aladdin), dioctyl phthalate (DOP, 98%, Aladdin) diethylenetriamine (99%, Aladdin), pure PVC (suspension grade, S-1000 ZnCl<sub>2</sub> (95%, Nanjing Chemical Reagent), sodium chloride (99%, Nanjing Chemical Reagent), sodium bicarbonate (99%, Nanjing Chemical Reagent), anhydrous magnesium sulfate (99%, Nanjing Chemical Reagent), tetrahydrofuran (THF, 99%, Nanjing Chemical Reagent), N,N-dimethyl-formamide (DMF, 99%, Nanjing Chemical Reagent), methanol (99%, Nanjing Chemical Reagent), and n-hexane (97%, Nanjing Chemical Reagent) were used as purchased.

### 2.2 Synthesis of Myrac Aldehyde (MA)

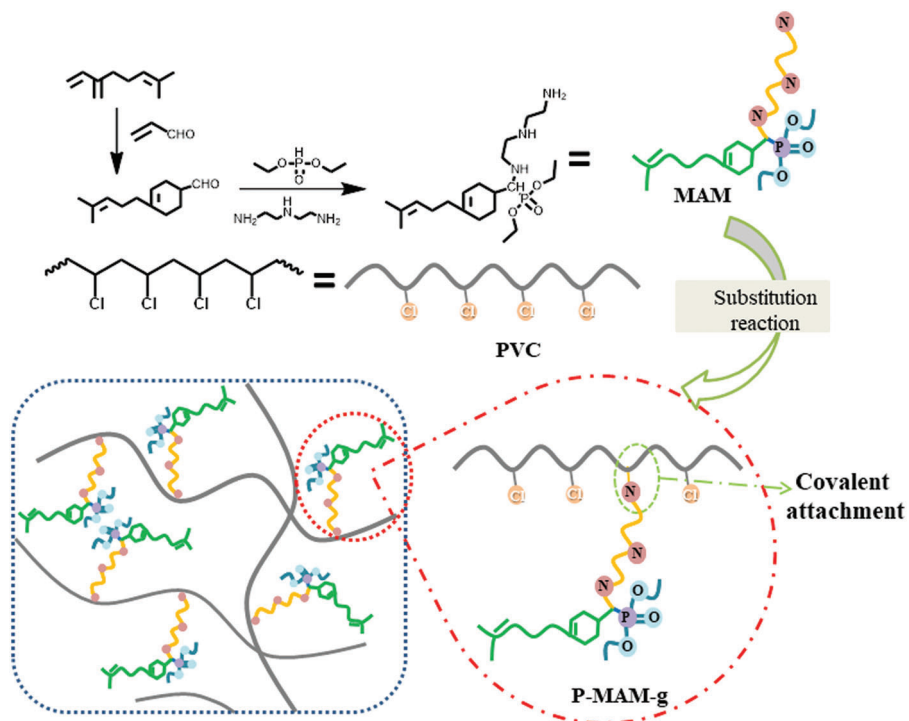
First, myrcene (55.85 g, 0.410 mol) and zinc chloride (3.41 g, 0.025 mol) were added into 250 mL flask equipped with the magnetic stirrer and reflux condenser. After the temperature was raised to 55°C, acrolein (27.47 g, 0.49 mol) was added dropwise and, maintained the temperature at approximately 55°C. The resulting suspension was aging at 60°C for 6 h. The obtained product was washed by 10% sodium chloride solution, 5% sodium bicarbonate, dried with anhydrous magnesium sulfate and removed the excess acrolein by a rotary evaporator to get a light yellow liquid (MA, Fig. 1).

### 2.3 Synthesis of Mannich Base Derived from Myrcene (MAM)

First, MA (28.85 g, 0.15 mol) was added dropwise to a flask containing diethylenetriamine (15.48 g, 0.15 mol) solution. The mixture was stirred at 20°C for 2 h and then raised to 90°C. Thereafter, the resulting mixture was raised to 90°C. Then diethyl phosphite (20.72 g, 0.15 mol) was added dropwise to the above mixture and kept at 90°C for 4 h. After the reaction, the product was raised to 120°C to remove water. Finally, a light-yellow slimy product was obtained (MAM).

### 2.4 Synthesis of MAM Grafted PVC (P-MAM-g)

A mixture (7 g) of PVC and MAM was dissolved in 80 mL of DMF, the resulted solution was washed with methanol several times and dried in a drybox at 60°C. The obtained product (5 g) was dissolved in THF (60 mL), then poured into a glass dish and dried at room temperature for 2 days to get the self-plasticization PVC materials (P-MAM-g) [21]. All the P-MAM-g (P-MAM-1, P-MAM-2, P-MAM-3, and P-MAM-4) were synthesized by the same reaction conditions as described above, except that the mass ratios of PVC and MAM were 5:1, 5:2, 5:3, 5:4, respectively. Pure PVC and PVC/40DOP [m(PVC):m(DOP) = 2.5] samples were prepared by the same method.



**Figure 1:** Preparation of mannich base originated from myrcene (MAM) grafted PVC (PVC-MAM-g)

### 2.5 Molecular Structure Characterization

Fourier transform infrared (FT-IR) spectra were achieved from Nicolet iS10 FT-IR (Nicolet Instrument Corp., USA) infrared spectrophotometer by the KBr disc method.

<sup>1</sup>H NMR test was performed on a Bruker 400 MHz spectrometer (Bruker, Rheinstetten, Germany). CDCl<sub>3</sub> was used as a solvent to dissolve the samples of MA and MAM, respectively. Deuterated dimethyl sulfoxide (DMSO) was used as a solvent to dissolve the samples of PVC P-MAM-2 and P-MAM-4, respectively.

Weight-average molecular weight and dispersity were measured using a gel permeation chromatograph (GPC) made by Waters, USA at 30°C (flow rate: 1 mL min<sup>-1</sup>, column: mixed PL gel 300 × 718 mm and 25 μm, HPLC-grade DMF as solvent) using. All PVC materials were dissolved in THF solutions to form a concentration of 1~5 mg mL<sup>-1</sup>.

### 2.6 Thermal Stability Analysis

The static thermal aging test was performed according to ISO 305-1990 (E) (Plastics. 1990). The PVC sheet was cut into 20 mm × 20 mm pieces and put in a thermal aging test box at 180°C. The color of the sample was recorded every 5 min, and then the thermal stability of the sample could judge by the degree of color change.

The thermogravimetric analysis (TGA) was also performed by a TA Q600 instrument (NetzschInstrument Corp., Germany). Typically, 4 mg of samples were heated from 40 to 600°C at a heating rate of 10 °C min<sup>-1</sup>, under nitrogen flow (100 mL min<sup>-1</sup>).

### 2.7 Mechanical Properties Analysis

Differential scanning calorimetry (DSC) measurement was measured on a TA Instrument (NETZSCH DSC 200 PC) in a nitrogen atmosphere. The measurement temperature range is from -50 to 120°C with a heating rate of 20°C min<sup>-1</sup>. Approximately 5~10 mg of PVC and self-plasticization PVC materials were

weighed and sealed in a 40  $\mu\text{L}$  aluminum crucible and immediately detected using DSC measurement. The DSC data was collected from the first cycle of heating.

Tensile strength and elongation at break were carried out according to the American Society for testing and materials (ASTM D638-03), and recorded on a CMT4303 universal test machine (Sans, China). The cross head speed was 50  $\text{mm min}^{-1}$ . The samples used in the tensile test were 0.47 mm thick, 3.98 mm wide and 25 mm long. At least five tests were repeated for each sample.

DMTA Q800 (TA Instruments, USA) was used to analyze the dynamic mechanical behavior of the PVC sample under the tension mode. The oscillatory frequency used in the dynamic test was 1 Hz. The temperature range was within  $-80$ – $120^\circ\text{C}$  with a temperature rate of  $3^\circ\text{C min}^{-1}$ .

### 2.8 Migration Properties Analysis

The migration resistance ability of the samples was investigated via the leaching experiment according to the ASTM D5227. Typically, the PVC sample ( $2 \times 2 \times 0.45 \text{ cm}^3$ ) with precise mass was immersed in n-hexane and kept at  $50^\circ\text{C}$  for 2 h. And PVC sample ( $2 \times 2 \times 0.45 \text{ cm}^3$ ) with precise mass was immersed in deionized water and kept at  $25^\circ\text{C}$  for 24 h. Subsequently, the above sample was thoroughly washed with deionized water, dried and weight for a second time. Degree of migration (%) =  $\frac{W_{\text{before}} - W_{\text{after}}}{W_{\text{before}}} \times 100$ .  $W_{\text{before}}$  is the weight of the sample before test.  $W_{\text{after}}$  is the weight of the sample after the test. Besides, the  $T_g$  of extracted samples were determined by DSC from  $-50$  to  $120^\circ\text{C}$  at a heating rate of  $20^\circ\text{C min}^{-1}$ .

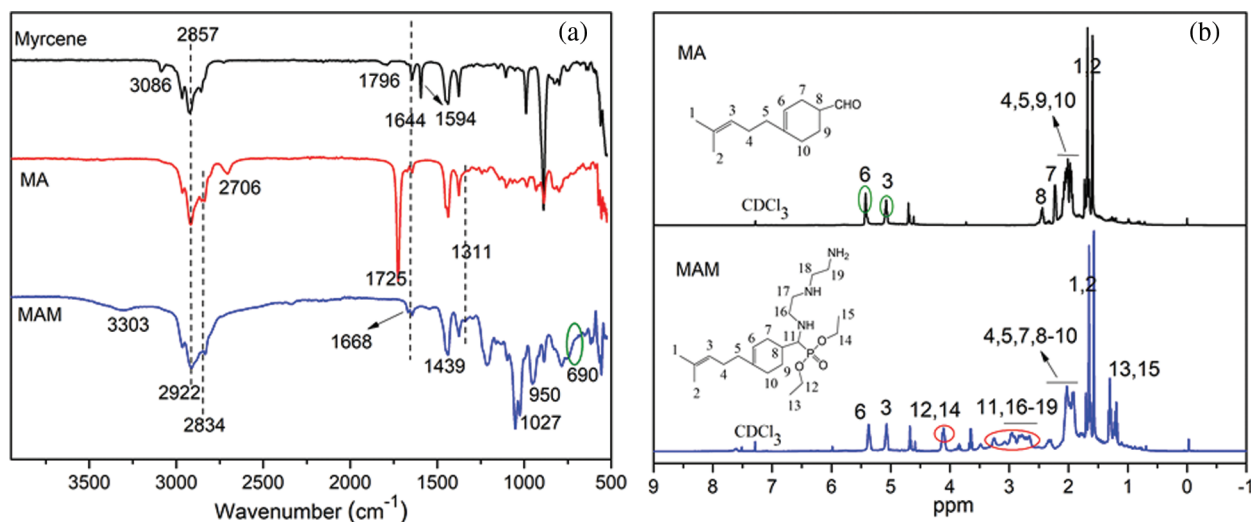
## 3 Results and Discussion

### 3.1 Synthesis and Characterization

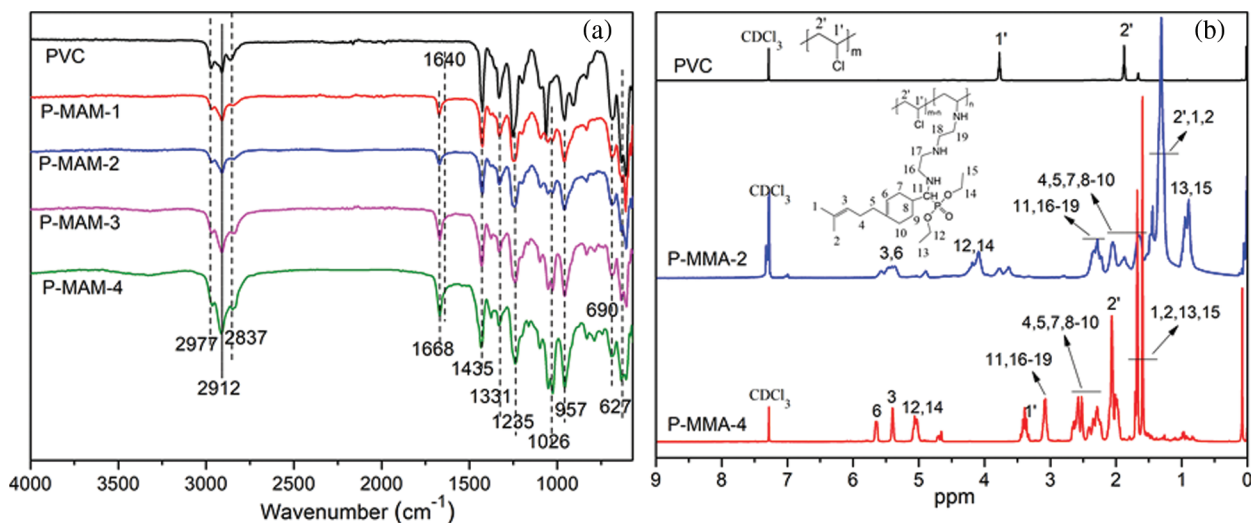
The structures of the as-prepared products were characterized and confirmed by FT-IR and  $^1\text{H-NMR}$  spectroscopy. Fig. 2a shows the FT-IR spectra of myrcene, MA, and MAM. After the reaction of myrcene and acrolein, the absorption peaks representing conjugated double bonds ( $1594 \text{ cm}^{-1}$ ) and the terminal vinyl group of myrcene ( $3086$  and  $1796 \text{ cm}^{-1}$ ) disappeared. In addition, the resulting product showed the peaks for aldehyde groups ( $1725 \text{ cm}^{-1}$ ) and C–H bonds in the hexatomic ring ( $2706$  and  $1311 \text{ cm}^{-1}$ ). The double bond absorption peak ( $1644 \text{ cm}^{-1}$ ) was retained, indicating the successful preparation of MA. In the FTIR spectrum of the mannich reaction adduct, the peaks representing aldehyde groups ( $1725 \text{ cm}^{-1}$ ) disappeared and the peaks representing P=O, C–N and P–O ( $1439$ ,  $1027$  and  $950 \text{ cm}^{-1}$ ) appeared after the reaction of MA, diethyl phosphite and diethylenetriamine, suggesting successful preparation of MAM. A deep insight into the chemical structures of MA and MAM was further obtained by  $^1\text{H NMR}$  characterization [Fig. 2b]. In comparison with MA, the MAM spectrum showed several new peaks in the approximately 4.5–2.5 ppm range (peaks 11, 12, 14, and 16–19), attributing to the hydrogen in the methylene connected to N or O containing groups such as  $-\text{CH-NH}-$ ,  $\text{P-O-CH}_2-$ , and  $-\text{NH-CH}_2-\text{CH}_2-\text{NH}-$ . This indicates that diethyl phosphite and diethylenetriamine were successfully introduced into the structure of MA. Moreover, other characteristic peaks of MA such as methyl (peaks 1 and 2) and methylene (peaks 3 and 6) were well-preserved. The FT-IR and  $^1\text{H NMR}$  results demonstrate successful preparation of MAM.

MAM was covalently bonded to PVC via nucleophilic replacing the unstable chlorine atoms of PVC chains. The functional groups of the as-prepared samples were investigated by FT-IR spectroscopy. The peaks at  $2977$ ,  $2912$ ,  $2837$ ,  $1668$ ,  $1026$ ,  $950$ , and  $690 \text{ cm}^{-1}$  (Fig. 3a) were assigned to the C–H ( $\text{sp}$ ), C–H ( $\text{sp}^3$ ), C–H ( $\text{sp}^2$ ), N–H stretching vibrations, C–N, P–O, and N–H rocking vibrations, respectively. The intensity of the peaks at  $1668$ ,  $1026$ ,  $950$ , and  $690 \text{ cm}^{-1}$  increased with the increasing replacement of chlorine atoms with MAM in PVC. In addition, the intensity of the peaks at approximately  $627 \text{ cm}^{-1}$ , assigned to the C–Cl stretching vibration of PVC, gradually decreased with increasing replacement of chlorine atoms with MAM, indicating successful preparation of P-MAM-g. The chemical structures of

PVC and P-MAM-g were also investigated by  $^1\text{H}$  NMR. As shown in Fig. 3b, P-MAM-2 and P-MAM-4 show several new peaks in the ranges of 2.0–5.5 ppm (peaks 11, 12, 14, and 16–19) in comparison with PVC. These typical peaks are also be found in MAM, indicating the successful introduction of MAM into the PVC structure. Moreover, the intensity of these signals increased with the increasing displacement of chlorine in the PVC structure, while the intensity of other characteristic peaks such as  $-\text{CH}-\text{Cl}$  (peak 1') and  $\text{CH}_2$  (peak 2') gradually decreased, indicating successful preparation of P-MAM-g.



**Figure 2:** (a) FT-IR spectra of myrcene, MA, and MAM; (b)  $^1\text{H}$  NMR spectra of MA and MAM




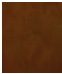








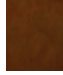




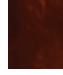




**Figure 3:** (a) FT-IR spectra of pure PVC and P-MAM-g; (b)  $^1\text{H}$  NMR spectra of pure PVC, P-MAM-2, and P-MAM-4

The number average molecular weight ( $M_n$ ) of the as-prepared P-MAM-g samples was studied by gel permeation chromatography (GPC), as displayed in Fig. S1 and Table S1. The  $M_n$  increased from 28,048 to 28,851 g/mol with increasing replacement of chlorine atoms. These results demonstrate that the chlorine atoms in PVC were successfully substituted with mannich base derived from myrcene.

### 3.2 Thermal Stability Evaluated by Discoloration

In the process of heating treatment, the DHC of PVC unavoidably results in unacceptable discoloration. To comprehensively investigate the thermal stability of the PVC materials described above, the color stability was measured with a thermal aging test at 180°C (Table 1). The pure PVC strips initially exhibited excellent color, but turned dark brown in 5 min, and absolute black within 15 min. This phenomenon is derived from the degradation of pure PVC in the thermal treatment process. During this process, the chloride anions originating from the C–Cl bond breaking can extract protons from the adjacent C–H bond, eliminating HCl from the PVC chains. The loss of HCl forms conjugated unsaturated double bonds sequences, causing the color change of the polymer from white to slight yellow, dark brown, and finally absolute black [22]. The initial color of the P-MAM-g materials was tan or light brown. The thermal aging tests of the P-MAM-g samples show that at 5 min, all four P-MAM-g materials had a tawny brown color, lighter than the dark brown displayed by pure PVC at 5 min. The sample with the smallest change in color was P-MAM-3. Moreover, after 15 min, P-MAM-3 remained dark brown instead of turning completely black, unlike pure PVC or the other P-MAM-g materials. These results indicated that the covalent attachment of MAM to PVC improved the initial and long-term stability of PVC. This phenomenon can potentially be attributed to the double bonds of P-MAM-g, replacing active chlorine atoms and reacting with the unstable macromolecular radical of PVC, thus enhancing stability. In addition, the multiple double bonds of P-MAM-g assisted the formation of stable conjugated polyene compounds, further restraining the deterioration of PVC samples.

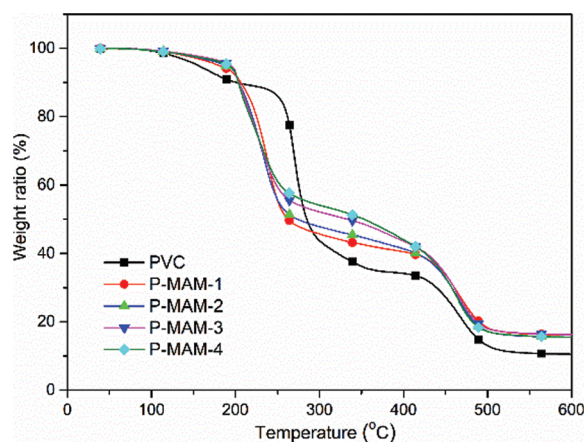
**Table 1:** Color changes of pure PVC and P-MAM-g samples under thermal aging at 180°C

Sample	Color of sample at thermal aging time (min)			
	0	5	10	15
PVC				
P-MAM-1				
P-MAM-2				
P-MAM-3				
P-MAM-4				

### 3.3 Thermal Stability Evaluated by TGA

The additional insight into the thermal stability and thermal degradation behavior of pure PVC and P-MAM-g was obtained by thermogravimetric analysis (TGA) in an N<sub>2</sub> atmosphere. Fig. 4 shows that the thermal decomposition behavior of all PVC materials can be divided into two stages in good agreement with previously reported results [23,24]. The first stage (200–400°C) is mainly attributed to the release of hydrogen chloride leading to the generation of conjugated polyene structures. The second stage (400–560°C) is caused by the formation of aromatic compounds due to the cyclization of conjugated polyene sequences. All the relevant information is listed in Table 2.  $T_5$  is the temperature at 5% weight

loss,  $T_{\max 1}$  and  $T_{\max 2}$  correspond to the temperatures at the maximum weight loss rate in the first and second degradation stages, respectively, while  $W_{300}$  and  $W_{600}$  are associated with the yields of residue at 300 and 600°C, respectively. The  $T_5$  and  $W_{600}$  values of pure PVC were 154.2°C and 10.53%, respectively, while the  $T_5$  and  $W_{600}$  values for P-MAM-g were 179.2–194.2°C and 15.44%–16.23%, respectively. Compared to the PVC samples, the grafted PVC samples show higher  $T_5$ , the maximum weight loss rate of the first degradation, and  $W_{600}$ . These results demonstrate that P-MAM-g has enhanced initial and long-term thermal stability compared with pure PVC. Moreover, P-MAM-3 demonstrates enhanced thermal stability among the P-MAM-g materials. These results match those of the thermal aging test at 180°C.



**Figure 4:** TGA curves of pure PVC and P-MAM-g

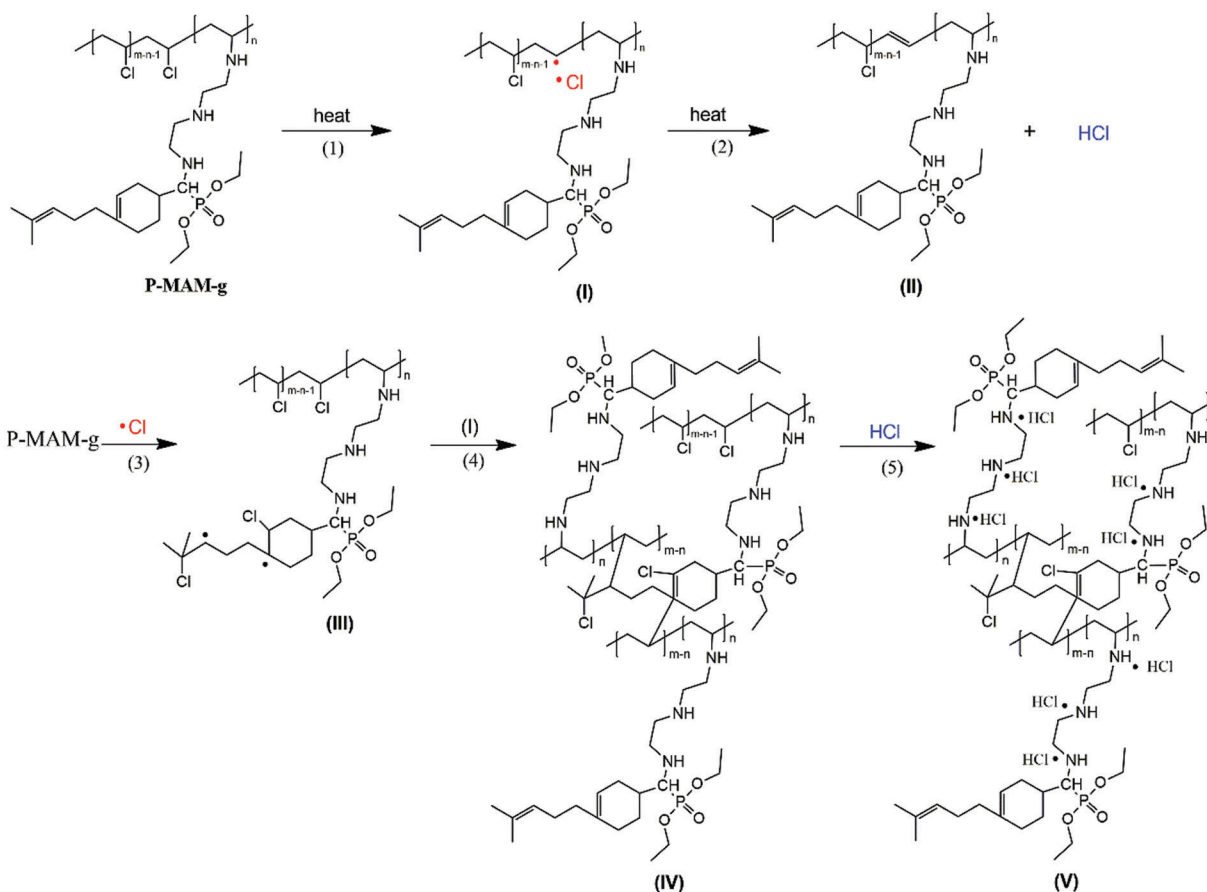
**Table 2:** Eigenvalues of the TGA curves of pure PVC and P-MAM-g

Sample	$T_5$ (°C)	$T_{\max 1}$ (°C)	$W_{300}$ (%)	$T_{\max 2}$ (°C)	$W_{600}$ (%)
Pure PVC	154.2	270.3	43.89	464.9	10.53
P-MAM-1	179.2	238.9	45.71	459.7	16.09
P-MAM-2	189.2	233.9	47.85	464.0	15.44
P-MAM-3	194.2	228.7	52.17	463.6	16.23
P-MAM-4	191.7	206.8	54.16	462.7	15.52

### 3.4 Thermal Stabilization Mechanism of P-MAM-g

Pure PVC sample tends to degrade under the processing temperature of 180°C. A potential degradation mechanism can be described as follows: the chloride anion produced by the C–Cl bond breaking extracts hydrogen from the adjacent C–H bond, eliminating HCl from the PVC chain. The loss of HCl results in the formation of conjugated double bonds sequences, causing the color change of the polymer from white to light yellow, dark brown, and finally completely black. As illustrated in Fig. 5, the generally accepted stabilization mechanism is based on the phenomena of P-MAM-g double bonds acting as radical trap reagents. In addition, the amino groups can absorb HCl to improve the stabilization of P-MAM-g. During the induction period of degradation (i.e., 0, 10, 20, 30, and 40 min), the Cl radicals originated from P-MAM-g degradation react with the double bond of P-MAM-g to form the radical **III**. Next, **III** captures the P-MAM-g radicals (**I**) to produce **IV**. Subsequently, **IV** captures the HCl eliminated from PVC. The process of capturing radicals and HCl continues until large amounts of conjugated polyene appear in the P-MAM-g molecules.





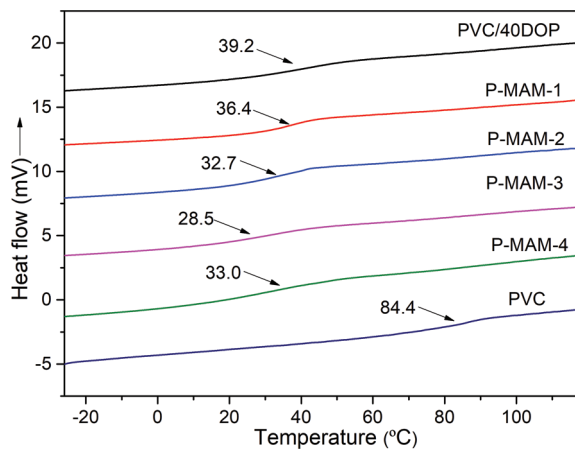
**Figure 5:** Proposed stabilization mechanism of P-MAM-g

### 3.5 Mechanical Properties

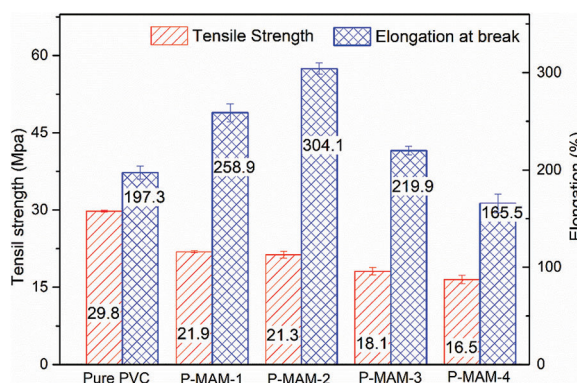
In addition to thermal aging, the thermal DHC of PVC materials can also deteriorate their mechanical properties [25]. The  $T_g$  of P-MAM-g was studied by DSC and compared with the  $T_g$  of pure PVC and a non-covalent mixture of PVC/40DOP. As displayed in Fig. 6, the  $T_g$  values of PVC/40DOP, P-MAM-1, P-MAM-2, P-MAM-3 and P-MAM-4 were 39.2°C, 36.4°C, 32.7°C, 28.5°C, and 33.0°C, respectively, far lower than the  $T_g$  value of pure PVC (84.4°C) [17]. P-MAM-g demonstrated an improved plasticization ability in comparison to PVC/40DOP and pure PVC. Grafting ester group, hexatomic ring and longer alkyl chains simultaneously onto PVC decreased the polymer-polymer interaction and enhanced the free volume between polymer molecules, which is helpful for decreasing the  $T_g$  of P-MAM-g [26–28]. The above analysis verifies that the introduction of multifunctional mannich base derived from myrcene into PVC is an effective strategy for providing PVC with intrinsic plasticization abilities.

The tensile strength of P-MAM-g was characterized to evaluate its mechanical properties. Fig. 7 shows that the tensile strength of P-MAM-g tends to decrease with increasing levels of MAM. This phenomenon may originate from the fact that MAM acts as a lubricant in PVC, weakening the internal friction between the PVC chains. Among the grafted PVC, P-MAM-2 exhibited the largest elongation at break (304.1%), which is 1.54 times higher than that of pure PVC. This may be attributed to the covalent bond between MAM and PVC, which can maintain the uniform and optimal structure of the material under tensile, preventing crack propagation and enabling the molecular chains to extend maximally [29]. These results further indicate that the covalent bond between MAM and PVC plays an important role in obtaining PVC

materials with high flexibility and extensibility. This characterization is in strong agreement with the DSC results.



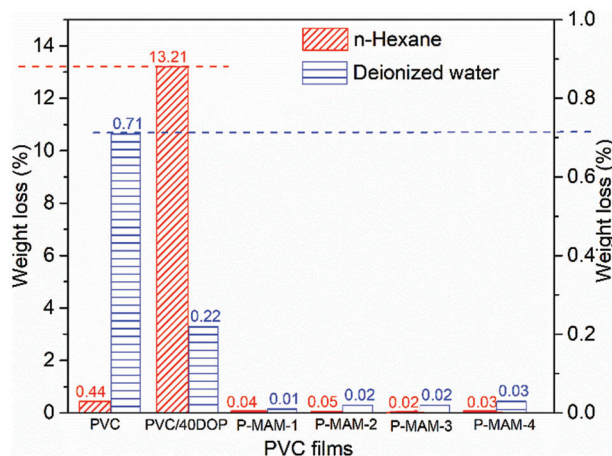
**Figure 6:** DSC curves of P-MAM-g



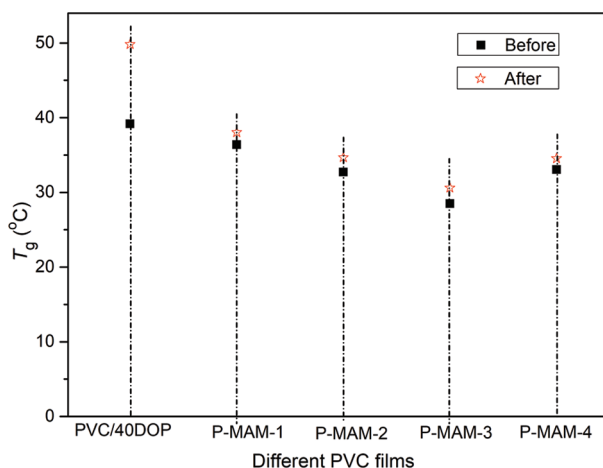
**Figure 7:** Tensile properties of P-MAM-g

### 3.6 Migration Resistance Properties

The migration resistance ability is an important criterion for assessing the performance of PVC materials [30] and was investigated via the leaching test in this study according to ASTM procedures. As illustrated in Fig. 8, PVC/40DOP displayed 13.21% and 0.22% of the migration ability of compounds, respectively, indicating its poor anti-migration ability. However, the leaching tests showed that the migration of all P-MAM-g samples was almost negligible, indicating the outstanding anti-migration ability of P-MAM-g ascribed to the covalent bond between PVC and MAM [31]. As shown in Fig. 9, no considerable changes in the  $T_g$  of the P-MAM-g were observed, and the  $T_g$  values were below 38°C after the leaching experiment. Under the same experimental conditions, the  $T_g$  of PVC/40DOP remarkably raised from 39.2 to 49.9°C. Therefore, compared with PVC/40DOP, P-MAM-g films demonstrated improved organic functional component anti-migration ability and retained their flexibility at room temperature.



**Figure 8:** Weight loss of PVC/40DOP and P-MAM-g migration after the leaching test



**Figure 9:**  $T_g$  of the P-MAM-g before and after leaching test in n-Hexane

#### 4 Conclusion

A series of self-stabilized PVC materials (P-MAM-g) were obtained by replacing chlorine in PVC with a mannich base derived from myrcene. The thermal stability, mechanical properties, and migration resistance ability of P-MAM-g were determined by TGA, thermal aging, DSC, and tensile tests. The thermal aging tests demonstrate that the best-performing P-MAM-3 material showed significantly less discoloration than the pure PVC after 15 min at 180°C, turning brown instead of completely black. In the TGA experiments, the temperature at 5% weight loss was 154.2°C and the residue yield at 600°C was 10.53%, whereas the two parameters for P-MAM-g were in the range 179.2–194.2°C and 15.44%–16.23%. These results demonstrate that covalent attachment of MAM to PVC improved the initial and long-term stability of PVC materials. This enhanced performance was attributed to the grafting of the double bonds and amino groups, that can simultaneously trap PVC radicals and HCl resulting from PVC deterioration onto the architecture of P-MAM-g. The DSC results revealed that P-MAM-g had improved plasticization performance compared with a non-covalent mixture of PVC and DOP. P-MAM-g also demonstrated an improved anti-migration ability of organic functional components compared with PVC/40DOP and retained their flexibility at room temperature. In the tensile tests, P-MAM-2 exhibited the highest elongation at break value (304.08%), 1.54 times higher than that of pure PVC. The tensile experiments

further showed that the covalent bond between MAM and PVC plays an important role in obtaining PVC materials with self-stabilization, high flexibility, and stretch ability.

**Acknowledgement:** This study was financially supported by the National Natural Science Foundation of China (21905117) and the Priority Academic Program Development of Jiangsu Higher Education Institutions (PAPD).

**Funding Statement:** This work was subsidized for the National Natural Science Foundation of China (21905117) and the Priority Academic Program Development of Jiangsu Higher Education Institutions (PAPD).

**Conflicts of Interest:** The authors declare that they have no conflicts of interest to report regarding the present study.

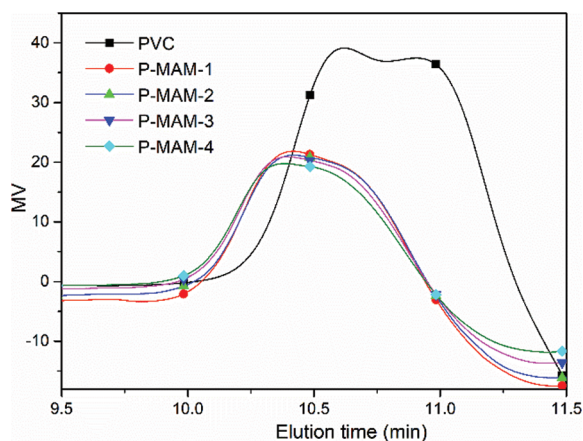
## References

1. Hipolito, V. L., Amorim, V. A., Gleize, P. J. P., Giroto, E., Júnior, A. C. et al. (2022). Techno-economic-environmental characteristics of polyurethane composite to thermal insulation for building with flame resistance: Corroborative effect recycled of PVC and aluminum oxide. *Journal of Material Cycles and Waste Management*, 24(2), 452–465. DOI 10.1007/s10163-021-01326-0.
2. Funari, M. F., Spadea, S., Lonetti, P., Lourenço, P. B. (2021). On the elastic and mixed-mode fracture properties of PVC foam. *Theoretical and Applied Fracture Mechanics*, 112(4), 102924. DOI 10.1016/j.tafmec.2021.102924.
3. Yu, J., Sun, L., Ma, C., Qiao, Y., Yao, H. (2016). Thermal degradation of PVC: A review. *Waste Management*, 48, 300–314. DOI 10.1016/j.wasman.2015.11.041.
4. Gama, N., Santos, R., Godinho, B., Silva, R., Ferreira, A. et al. (2019). Triacetin as a Secondary PVC Plasticizer. *Journal of Polymers and the Environment*, 27(6), 1294–1301. DOI 10.1007/s10924-019-01432-z.
5. Li, M., Li, S. H., Xia, J. L., Ding, C. X., Wang, M. et al. (2017). Tung oil based plasticizer and auxiliary stabilizer for poly(vinyl chloride). *Materials and Design*, 122, 366–375. DOI 10.1016/j.matdes.2017.03.025.
6. Shi, Y. Q., Wang, Y. T., Ma, B., Ma, M., Chen, S. et al. (2019). Tensile properties, thermal stability, and the mechanism of PVC stabilized with zinc and calcium oxolinic complexes. *Journal of Applied Polymer Science*, 136(4), 47004. DOI 10.1002/app.47004.
7. Thirupathiah, G., Satapathy, S., Palanisamy, A. (2019). Studies on epoxidised castor oil as co-plasticizer with epoxidised soyabean oil for PVC processing. *Journal of Renewable Materials*, 7(8), 775–785. DOI 10.32604/jrm.2019.06399.
8. Li, D. L., Liu, S., Gu, L. Q., Li, G. H., Ding, Y. et al. (2021). Preparation of rare earth complexes with curcumin and their stabilization for PVC. *Polymer Degradation and Stability*, 184(1), 109480. DOI 10.1016/j.polymdegradstab.2020.109480.
9. Li, X., Nie, X., Chen, J., Wang, Y., Li, K. (2017). Synthesis and application of a novel epoxidized plasticizer based on cardanol for poly(vinyl chloride). *Journal of Renewable Materials*, 5(2), 154–164. DOI 10.7569/JRM.2017.634101.
10. Li, M., Zhang, J. W., Xin, J. N., Huang, K., Li, S. H. et al. (2017). Design of green zinc-based thermal stabilizers derived from tung oil fatty acid and study of thermal stabilization for PVC. *Journal of Applied Polymer Science*, 134(14), 44679. DOI 10.1002/app.44679.
11. Ye, F., Guo, X. J., Zhan, H. H., Lin, J. X., Lou, W. C. et al. (2018). The synergistic effect of zinc urate with calcium stearate and commercial assistant stabilizers for stabilizing poly(vinyl chloride). *Polymer Degradation and Stability*, 156, 193–201. DOI 10.1016/j.polymdegradstab.2018.08.012.
12. Ma, Y. F., Liao, S. L., Li, Q. G., Guan, Q., Jia, P. Y. et al. (2020). Physical and chemical modifications of poly(vinyl chloride) materials to prevent plasticizer migration-Still on the run. *Reactive and Functional Polymers*, 147(45), 104458. DOI 10.1016/j.reactfunctpolym.2019.104458.

13. Wang, M., Xia, J. L., Jiang, J. C., Li, S. H., Li, M. (2016). Mixed calcium and zinc salts of N-(3-amino-benzoic acid)terpene-maleamic acid: Preparation and its application as novel thermal stabilizer for poly(vinyl chloride). *RSC Advances*, 6(99), 97036–97047. DOI 10.1039/C6RA19523G.
14. Jia, P. Y., Hu, L. H., Shang, Q. Q., Wang, R., Zhang, M. (2017). Self-plasticization of PVC materials via chemical modification of mannich base of cardanol butyl ether. *ACS Sustainable Chemistry & Engineering*, 5(8), 6665–6673. DOI 10.1021/acssuschemeng.7b00900.
15. Zhu, X. D., Li, K. S., Chen, F. (2017). Microwave assisted friedel-crafts grafting reaction of PVC with phenol and the effect on thermal stability of PVC. *Polymer Materials Science and Engineering*, 33, 7–13. DOI 10.16865/j.cnki.1000-7555.2017.04.002.
16. Wang, M., Li, S. H., Ding, H. Y., Xia, J. L., Li, M. et al. (2020). Construction of efficient tung-oil-based thermal stabilizers bearing imide and epoxy groups for PVC. *New Journal of Chemistry*, 44(11), 4538–4546. DOI 10.1039/C9NJ05777C.
17. Wang, M., Song, X. H., Jiang, J. C., Xia, J. L., Li, S. H. et al. (2017). Excellent hydroxyl and nitrogen rich groups-containing tung-oil-based Ca/Zn and polyol stabilizers for enhanced thermal stability of PVC. *Thermochimica Acta*, 658, 84–92. DOI 10.1016/j.tca.2017.10.008.
18. Yang, X. J., Wang, C. P., Li, S. H., Huang, K., Li, M. et al. (2017). Study on the synthesis of bio-based epoxy curing agent derived from myrcene and castor oil and the properties of the cured products. *RSC Advances*, 7(1), 238–247. DOI 10.1039/C6RA24818G.
19. Yang, X. J., Wang, C. P., Xia, J. L., Mao, W., Li, S. H. (2017). Study on synthesis of novel phosphorus-containing flame retardant epoxy curing agents from renewable resources and the comprehensive properties of their combined cured products. *Progress in Organic Coatings*, 110, 195–203. DOI 10.1016/j.porgcoat.2017.01.012.
20. Yang, X. J., Li, S. H., Xia, J. L., Song, J., Huang, K. et al. (2015). Renewable myrcene-based UV-curable monomer and its copolymers with acrylated epoxidized soybean oil: Design, preparation, and characterization. *BioResources*, 10(2), 2130–2142. DOI 10.15376/biores.10.2.2130-2142.
21. Wang, M., Kong, X. H., Song, X. H., Chen, Y. L., Bu, Q. (2021). Construction of enhanced self-plasticized PVC via grafting with bio-derived mannich base. *New Journal of Chemistry*, 45(7), 3441–3447. DOI 10.1039/D0NJ05714B.
22. Wu, B. Z., Wang, Y. T., Chen, S., Wang, M. Y., Ma, M. et al. (2018). Bis-uracil based high efficient heat stabilizers used in super transparent soft poly(vinyl chloride). *Polymer Degradation and Stability*, 149(9), 143–151. DOI 10.1016/j.polymerdegradstab.2018.01.029.
23. Luo, X., Chu, H., Liu, M. (2020). Synthesis of bio-plasticizer from soybean oil and its application in poly(vinyl chloride) films. *Journal of Renewable Materials*, 8(10), 1295–1304. DOI 10.32604/jrm.2020.011026.
24. Al-Mosawi, A. (2021). A novel evaluation method for dehydrochlorination of plasticized poly(vinyl chloride) containing heavy metal-free thermal stabilizing synergistic agent. *Polymers for Advanced Technologies*, 32(8), 3278–3286. DOI 10.1002/pat.5339.
25. Jia, P. Y., Zhang, M., Liu, C. G., Hu, L. H., Feng, G. D. et al. (2015). Effect of chlorinated phosphate ester based on castor oil on thermal degradation of poly (vinyl chloride) blends and its flame retardant mechanism as secondary plasticizer. *RSC Advances*, 5(51), 41169–41178. DOI 10.1039/C5RA05784A.
26. Vassilev, D., Petkova, N., Koleva, M., Denev, P. (2018). Microwave synthesis of inulin acetate as potential bio-based additive for poly(vinyl chloride). *Journal of Renewable Materials*, 6(7), 707–714. DOI 10.32604/JRM.2018.00015.
27. Lieberzeit, P., Bekchanov, D., Mukhamediev, M. (2022). Polyvinyl chloride modifications, properties, and applications: Review. *Polymers for Advanced Technologies*, 33(6), 1809–1820. DOI 10.1002/pat.5656.
28. Jia, P. Y., Ma, Y. F., Song, F., Hu, Y., Zhang, C. Q. et al. (2019). Toxic phthalate-free and highly plasticized polyvinyl chloride materials from non-timber forest resources in plantation. *Reactive and Functional Polymers*, 144, 104363. DOI 10.1016/j.reactfunctpolym.2019.104363.
29. Jia, P. Y., Ma, Y., Kong, Q., Xu, L., Hu, Y. et al. (2019). Graft modification of polyvinyl chloride with epoxidized biomass-based monomers for preparing flexible polyvinyl chloride materials without plasticizer migration. *Materials Today Chemistry*, 13, 49–58. DOI 10.1016/j.mtchem.2019.04.010.

30. Jia, P. Y., Ma, Y. F., Song, F., Liu, C. G., Hu, L. H. et al. (2021). Renewable atom-efficient dendrimer-like acetate: from toxic tung oil to non-toxic plasticizers. *Materials Today Chemistry*, 21(15), 100518. DOI 10.1016/j.mtchem.2021.100518.
31. Mercea, P. V., Losher, C., Benz, H., Petrasch, M., Costa, C. et al. (2021). Migration of substances from unplasticized polyvinylchloride into drinking water. Estimation of conservative diffusion coefficients. *Polymer Testing*, 104, 107385. DOI 10.1016/j.polymertesting.2021.107385.

### Supporting Information



**Figure S1:** GPC spectra of pure PVC and of P-MAM-g

**Table S1:** Relative molecular mass and distribution of pure PVC and -MAM-g

PVC material	Number average molecular weight ( $M_n$ , g/mol)	Weight-average molecular weight ( $M_w$ , g/mol)	Z-average molecular weight ( $M_z$ , g/mol)	Dispersity ( $M_z/M_w$ , g/mol)
PVC	19381	22087	25362	1.1
P-MAM-1	28048	30598	33430	1.1
P-MAM-2	28548	30787	33908	1.1
P-MAM-3	28669	30952	34719	1.1
P-MAM-4	28851	31242	35885	1.1